Elucidating the Aggregation Number of Dopamine-Induced α-Synuclein Oligomeric Assemblies

Niels Zijlstra,[†] Mireille M. A. E. Claessens,[†] Christian Blum,[†] and Vinod Subramaniam[†‡*]
[†]Nanobiophysics, MESA+ Institute for Nanotechnology and [‡]Nanobiophysics, MIRA Institute for Biomedical Technology and Technical Medicine, University of Twente, Enschede, The Netherlands

ABSTRACT Conventional methods to determine the aggregation number, that is, the number of monomers per oligomer, struggle to yield reliable results for large protein aggregates, such as amyloid oligomers. We have previously demonstrated the use of a combination of single-molecule photobleaching and substoichiometric fluorescent labeling to determine the aggregation number of oligomers of human α-synuclein, implicated in Parkinson's disease. We show here that this approach is capable of accurately resolving mixtures of multiple distinct molecular species present in the same sample of dopamine-induced α-synuclein oligomers, and that we can determine the respective aggregation numbers of each species from a single histogram of bleaching steps. We found two distinct species with aggregation numbers of 15–19 monomers and 34–38 monomers. These results show that this single-molecule approach allows for the systematic study of the aggregation numbers of complex supramolecular assemblies formed under different aggregation conditions.

INTRODUCTION

The neuronal protein α-synuclein (aS) is an intrinsically disordered protein consisting of 140 amino acids (1). aS is considered to be at the basis of Parkinson's disease, a human neurodegenerative disease characterized by the formation of intraneuronal Lewy bodies and the loss of dopaminergic neurons (2). Although Lewy bodies are composed largely of fibrillar aggregates of aS (3), a number of studies show that oligomeric aggregates are significantly more cytotoxic than the fibrils, indicating that oligomers play an essential role in the disease mechanism (4–7).

Depending on the aggregation conditions, a variety of oligomeric species are found, differing in terms of structure, morphology, toxicity, and aggregation number, that is, the number of monomers forming an oligomer (7–11). Structural and biophysical information on the different oligomers is essential to understanding the aggregation process and determining whether there is a specific cytotoxic oligomeric species or whether oligomers in general cause cell death, but such information is scarce.

Conventional methods to determine the aggregation number of oligomeric protein aggregates, such as mass spectrometry and size-exclusion chromatography, have failed to yield reliable results for amyloid oligomers. Recently, we showed that single-molecule photobleaching in combination with substoichiometric labeling can be used to accurately determine the aggregation number of aS oligomers formed at high aS concentrations (12). In our method we fluorescently label a small fraction of the monomeric subunits, as opposed to conventional photobleaching where all monomeric subunits of the oligomer are fluorescently labeled.

Sequential photobleaching of all fluorescent labels incorporated in a single oligomer generates discrete steps in the fluorescence intensity. For conventional photobleaching, where all monomers are labeled, counting the number of steps directly provides the number of monomers per oligomer (13,14). However, it is impossible to accurately determine the number of photobleaching steps for oligomeric aggregates consisting of many labeled monomeric subunits. The intensity decrease converges to an exponentially decaying curve making the individual bleaching steps indistinguishable (15). Furthermore, a large number of fluorescent labels may influence the aggregation process, resulting in structurally and functionally different oligomeric aggregates.

These problems can be overcome by using substoichiometric labeling, where only a small fraction of the monomeric subunits is labeled. Aggregating a mixture of labeled and unlabeled monomers is a stochastic process that results in a distribution in the number of fluorescently labeled monomers per oligomer, even for homogeneous oligomers of the same aggregation number (see Fig. 1). The average number of fluorescent labels per oligomer and hence the average number of photobleaching steps, can be optimized by tuning the exact label density, that is, the ratio of labeled to unlabeled monomers at the initiation of the aggregation. As a result, we can accurately determine the number of photobleaching steps even for large protein aggregates. However, in contrast to conventional

Submitted July 2, 2013, and accepted for publication December 3, 2013.

*Correspondence: subramaniam@amolf.nl or v.subramaniam@utwente.nl

Vinod Subramaniam's present address is FOM Institute AMOLF, Science Park 104, 1098 XG Amsterdam, The Netherlands

Editor: David Eliezer.

0006-3495/14/01/0440/7 $2.00

http://dx.doi.org/10.1016/j.bpj.2013.12.009

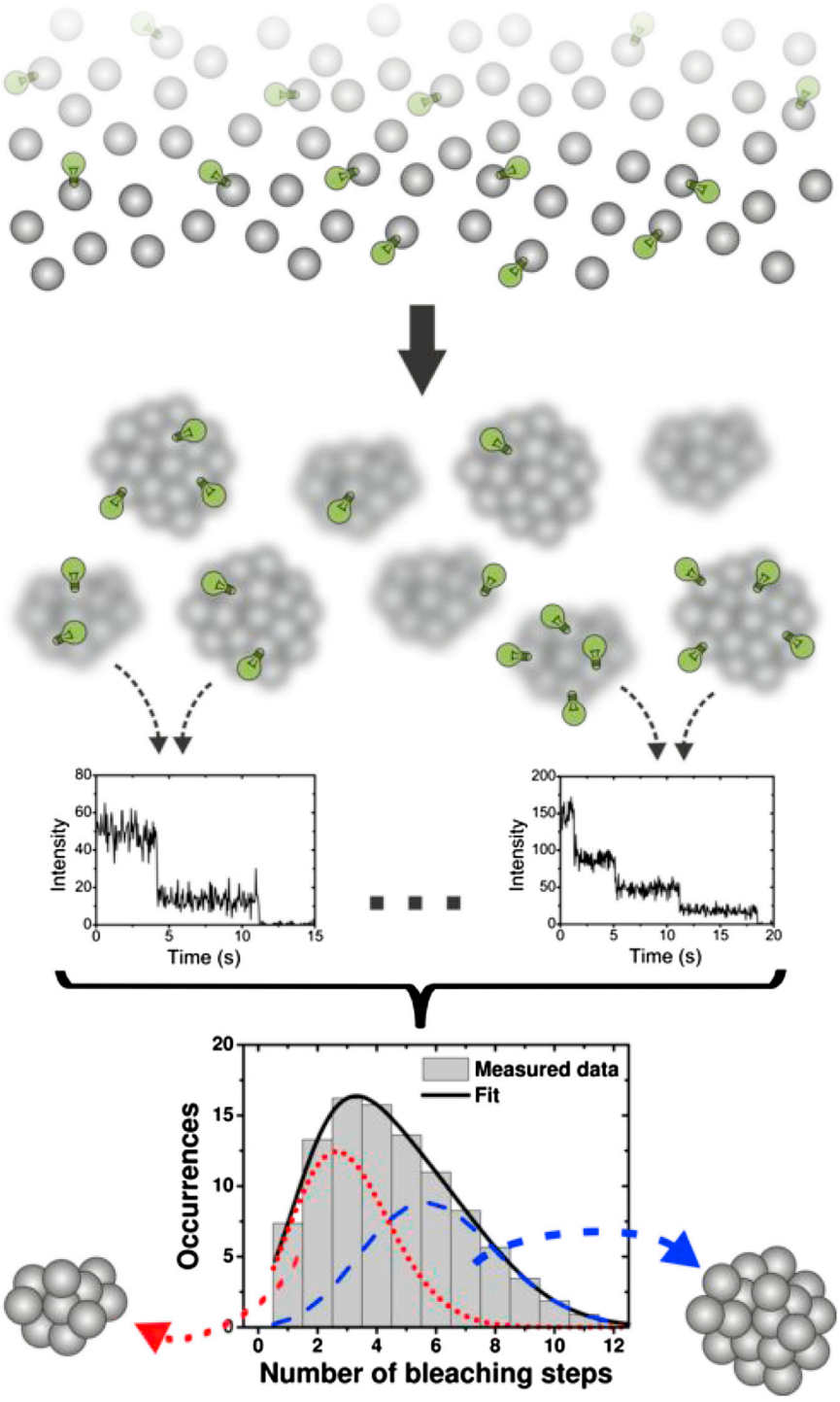

FIGURE 1 Using a substoichiometric mixture of fluorescently labeled and unlabeled monomers for aggregation will result in oligomers containing different numbers of fluorescently labeled monomers. Counting the number of bleaching steps for a statistically relevant number of oligomers will result in a distribution of bleaching steps that can be linked to the total number of monomers per oligomer via the label density chosen at the initiation of aggregation and the label PMF. If oligomers of different aggregation numbers are present, the measured histogram of bleaching steps will consist of the sum of binomial distributions. By fitting the appropriate number of species, it is possible to obtain the aggregation number of multiple species from a single histogram of bleaching steps. To see this figure in color, go online.

photobleaching, the number of observed bleaching steps from a single oligomer does not directly yield the number of monomers forming the oligomer due to the stochastic nature of aggregation. Now, the distribution in the number of fluorescent labels per oligomer is linked to the mean number of monomers per oligomer via the label density and the label probability mass function (PMF). The label PMF gives the probability that an oligomer with a defined number of monomers contains a specific number of labels. To accurately determine the aggregation number of the oligomer, it is essential to analyze a statistically relevant number of oligomers to determine the entire distribution in the number of labels per oligomer.

aS oligomers formed in the presence of dopamine are of special interest, because the selective loss of dopaminergic neurons suggests that dopamine plays a role in the formation of

cytotoxic aS oligomers (16). Previous studies by Conway et al. showed that the addition of dopamine can stabilize aS oligomers, preventing them from maturing into fibrils (17). Cappai et al. showed that dopamine accelerates the formation of non-amyloidogenic, sodium-dodecyl-sulfate-resistant aS oligomers (8). A range of biophysical techniques have been used to study the morphology of dopamine-induced oligomers, indicating a variety of different shapes and sizes (8,17,18), without providing insights into the exact aggregation number of these oligomers. Interestingly, there is considerable discussion about whether dopamine forms covalent or noncovalent bonds with the aS. Clearly, these interactions have an influence on the formation of the oligomers (17,19).

In this work, we study the aggregation number, or molecular composition, of dopamine-induced aS oligomers.

MATERIALS AND METHODS

Instrumentation and measurement procedure

The photobleaching experiments were performed using a custom-built inverted confocal microscope, similar to the one described in our previous study (12). In short, as excitation source, we used a pulsed diode laser (LDH-D-C-640, Picoquant, Berlin, Germany) operating at 640 nm at a repetition rate of 20 MHz. An epi-illumination configuration was used, i.e., the illumination and emission collection are through the same microscope objective (UPLSAPO 60×W, 60×, 1.2NA, Olympus, Center Valley, PA). The remaining excitation light in the detection path was suppressed with a long-pass filter (664 nm; Razoredge, Semrock, Rochester, NY) and a band-pass filter (Brightline, 708/75 nm; Semrock). The emission was spatially filtered using a 30 μm pinhole and was subsequently focused onto a single-photon avalanche diode (SPCM-APQR-16, PerkinElmer, Waltham, MA), connected to a photon counting module (PicoHarp300, Picoquant).

The initial scanning of the sample was done at a high scanning speed, 2 ms per pixel, and low excitation power, ~50 W/cm^2, to prevent dye bleaching. We then located individual oligomers in the initial area scan, see Section S1 in the Supporting Material, localized them in the focus of the microscope objective, and subsequently collected fluorescence intensity time traces from distinct oligomers. To record the time trace, we used higher excitation powers, ~750 W/cm^2, to make sure that each dye molecule photobleached. Typical time traces are shown in Section S2 in the Supporting Material.

α-Synuclein labeling, aggregation, and oligomer purification

Expression and purification of aS wild-type and mutant aS A140C was performed as previously described (19).

Before labeling, aS A140C in 10 mM Tris-HCl and 5 mM NaCl, pH 7.4, was reduced with a sixfold molar excess of dithiothreitol (DTT) for 30 min at room temperature. The samples were desalted using a Pierce Zeba desalting column. A twofold molar excess of Alexa Fluor 647 C2 maleimide (Life Technologies, Invitrogen, Carlsbad, CA) was added and incubated for 1 h in the dark at room temperature. Free label was removed using two consecutive desalting steps. The labeling efficiency was determined from the absorption spectrum. The protein concentration was determined from the absorbance at 276 nm using an extinction coefficient of 5745 M^{-1} cm^{-1}, and the Alexa Fluor 647 concentration from the absorbance at 650 nm using an extinction coefficient of 239,000 M^{-1} cm^{-1}. Subsequently, aS wild-type in 10 mM Tris-HCl, pH 7.4, was added to the labeled aS A140C to obtain the desired ratio between wild-type and A140C aS.

To prepare the aS oligomers, we optimized a protocol previously described in the literature to generate oligomers within an acceptable timeframe at the required yields (8). In short, the mixture of labeled and wild-type aS was dried in a vacuum evaporator and dissolved in 10 mM phosphate buffer, pH 7.4, at a final protein concentration of 140 μM. Dopamine was added at a final concentration of 200 μM and the solution was incubated for 3 h at 37°C. To protect the dopamine from light-induced degradation, we kept the sample in the dark during the entire aggregation time. To remove very large aggregates, the solution was filtered using a 0.22 μm spin filter. The oligomers were purified by size-exclusion chromatography on a Superdex200 gel filtration column using 10 mM Tris-HCl and 50 mM NaCl, pH7.4, as eluent. The fractions containing the aS oligomers were identified by the absorbance at both 276 nm and 650 nm. A typical elution profile is shown in Section S3 in the Supporting Material.

Sample preparation for single-molecule spectroscopy

Microscope glass coverslips were cleaned by placing them for at least 1 h in an ultraviolet/ozone cleaner (UV/Ozone ProCleaner Plus; Bioforce, San Diego, CA). The oligomers must be immobilized to be studied. To realize this, the isolated oligomers were diluted to ~1 nM in water and directly spin-coated for 10 s at 6000 rpm on top of a cleaned coverslip. The samples contained the oligomers at low concentrations, so that the oligomers were well separated and did not overlap within the diffraction limit of the microscope.

Fitting procedure

For the single species, the histograms of bleaching steps were fitted with a single binomial distribution given by

$$A \times \binom{n}{k} \times p^k \times (1-p)^{n-k}, \tag{1}$$

where A is the total number of events, n the number of trials, k the number of successes, and p the probability of success, which in this case is the same as the label density.

For the two- and three-species fit, a combination of binomials was used:

$$\sum_{i=1}^{n} A_i \times \binom{n}{k_i} \times p^{k_i} \times (1-p)^{n-k_i}. \tag{2}$$

All fitting was done using OriginPro 9.0 64-Bit.

RESULTS AND DISCUSSION

To study the aggregation number of dopamine-induced aS oligomers, we prepared Alexa Fluor 647 fluorescently labeled dopamine-induced oligomers with different label densities and analyzed bleaching traces for a minimum of 100 distinct oligomers per label density. To verify the stochastic incorporation of labeled aS into the oligomer, we compared the elution profiles of wild-type oligomers without fluorescent labels and the Alexa Fluor 647 labeled oligomers. We observe no difference in the peak position of the elution profile, and therefore conclude that the fluorescent label does not influence the aggregation process (see Section S4 in the Supporting Material).

Fig. 2 *a* shows the photobleaching histogram for dopamine-induced aS oligomers with a 20% label density built

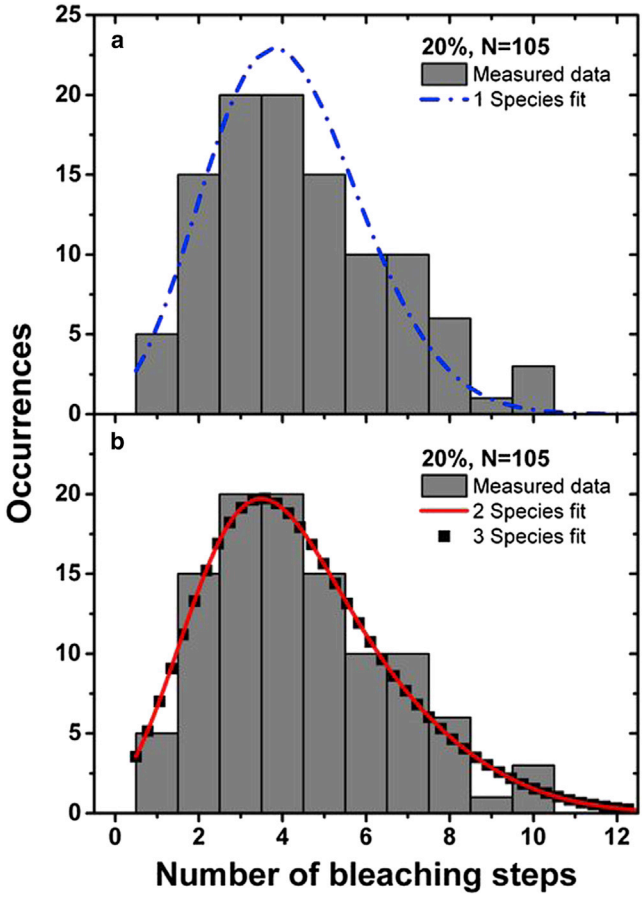

FIGURE 2 Experimental histograms of bleaching steps for dopamine-induced oligomers with a 20% label density built from bleaching traces of 105 distinct oligomers. (*a*) The histogram is fitted with a single (*blue dash-dotted line*) binomial distribution that does not represent the measured distribution accurately. (*b*) The histogram is fitted with a combination of two (*solid red line*) and three (*black squares*) binomial distributions that fit the histogram well. To see this figure in color, go online.

from bleaching traces analyzed for 105 distinct oligomers. The stochastic incorporation of labeled monomers in the oligomers is described by a classical Bernoulli process in which there is no preference for either labeled or unlabeled monomers. Assuming that there is only a single species of oligomer present, as seen before for oligomers prepared using a different protocol (12), the bleaching histogram was fitted with a single binomial distribution from which the average number of monomers per oligomer was obtained (Fig. 2 *a*, *blue dash-dotted line*). The fit, however, does not represent the data well. The histogram has a significantly lower peak value compared to the fit and displays a clear broadening, especially on the right side of the histogram.

The difference between the measured distribution and the fit is much larger than we observed previously for oligomers present in a single, well-defined species (12). Clearly, if the oligomers are present in multiple species instead of a single species, the distribution of bleaching steps will change significantly.

To test whether we can discriminate multiple species present in the same sample from a single histogram of bleaching steps, we simulated a histogram of bleaching steps for a mixture of two oligomeric species consisting of 20 and 35 monomers per oligomer (see Fig. 3). This histogram of bleaching steps consists of more than one binomial distribution. As a consequence, a single-species fit cannot adequately explain the histogram of bleaching steps (see Fig. 3, *black dash-dotted line*, for single-species fit). Compared to the single-species fit, the simulated histogram is clearly broadened, especially on the right side of the histogram, and has a lower peak value compared to the fit. The simulated histogram, however, can be adequately explained if a sum of multiple binomial distributions is fitted (see Fig. 3, *red solid line*). Moreover, this indicates that it is possible to obtain the aggregation number of multiple species from a single histogram of bleaching steps.

For the single-species fit of the experimental data corresponding to a 20% label density, we observe discrepancies similar to those seen for the single-species fit of the simulated histogram, suggesting that the dopamine-induced oligomers are composed of multiple species. A two-species fit of the experimental histogram of bleaching steps for the oligomers with 20% label density greatly improved the fit quality (see Fig. 2 *b*, *red solid line*), where both the peak height and the width of the histogram are now fitted well. The fit quality is characterized by the reduced χ-squared parameter (see Table 1). Upon adding a third species (Fig. 2 *b*, *black squares*), the algorithm finds two essentially identical species (17 and 18 monomers per oligomer), whereas the third species contains 32 monomers per oligomer. However, the three-species fit has a reduced fit quality compared to the two-species fit (see Table 1). We therefore

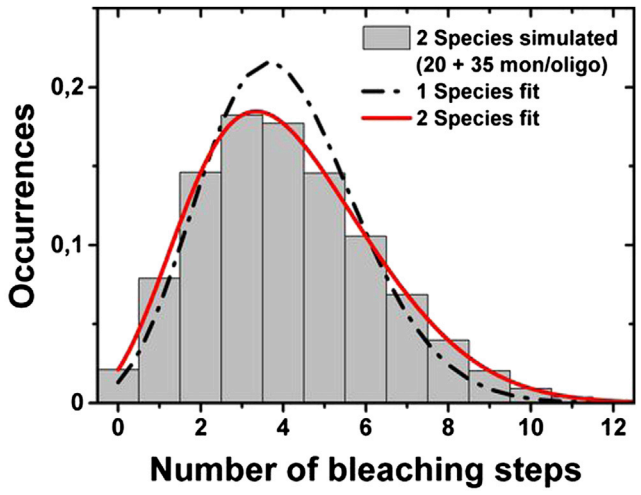

FIGURE 3 Simulated histogram of bleaching steps for a mixture of two oligomeric species consisting of 20 and 35 monomers per oligomer and present in equal fractions. The histogram is clearly broadened and has a lower peak value compared to the single-species fit (*black dash-dotted line*), whereas a two-species fit fully explains both the width and the height of the histogram. To see this figure in color, go online.

TABLE 1 Reduced χ-squared parameter for the one-, two-, and three-species fits and corresponding aggregation numbers of the oligomers

	Reduced χ-squared parameter	Aggregation number
1 species	4.8	21
2 species	2.1	17/31
3 species	2.6	17/18/32

conclude that two distinct oligomeric species are sufficient to explain the data fully.

When using the combination of single-molecule photobleaching and substoichiometric labeling, it is very important to use label densities for which the technique works optimally (12). Difficulties arise when using a label density that is either too low or too high. Choosing the appropriate label density becomes even more important if the oligomers are present in multiple species. Since both species have a different aggregation number, the label density has to be chosen in such a way that both aggregation numbers can be determined accurately.

To determine the optimal label density, we have to consider the following for both species. When using a lower label density, an increasing fraction of the oligomers will not contain a fluorescent label due to the stochastic nature of aggregation and are therefore invisible to this method. Because this fraction cannot be measured, it is not included in the histogram and will cause an uncertainty in the fitting. The larger the fraction of oligomers without a label, the larger is the uncertainty in the fitting, resulting in an overestimation of the number of monomers per oligomer. Clearly, for a two-species system, overestimating the aggregation number of the smaller species will also influence the aggregation number found for the larger species.

On the other hand, using a too-high label density will result in problems similar to those encountered with conventional photobleaching. The intensity decay will converge to an exponentially decaying curve, making it impossible to accurately determine the number of bleaching steps. As a consequence, those oligomers containing too many labels will not be included in the histogram, resulting in an underestimation of the number of monomers per oligomer.

To obtain optimal results, it is thus necessary to choose the label density in such a way that neither species suffers from either of these biases. To verify that the 20% label density we used is within the optimal range of label densities and hence gives accurate results for the aggregation number of both species, we also determined the photobleaching histograms for dopamine-induced aS oligomers with label densities of 15% and 10%, each built from bleaching traces of at least 100 distinct oligomers (see Fig. 4). There is, as expected, a clear shift of the histograms to a lower number of bleaching steps with decreasing label density, since a lower label density results in a lower average number of labels per oligomer. Each label density was fitted with a combination of two binomial distributions, and the mean

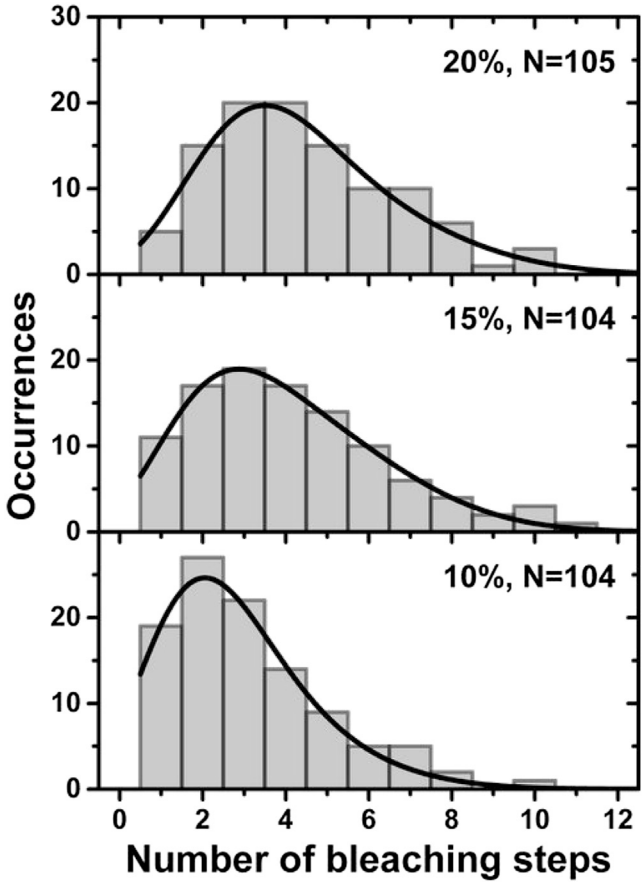

FIGURE 4 Histogram of bleaching steps for dopamine-induced oligomers with a 20%, 15%, and 10% label density, each built from bleaching traces of at least 100 distinct oligomers. The histograms are fitted with a combination of two binomial distributions (*solid black lines*). The mean values of the two binomial distributions give the mean numbers of monomers per oligomer for both species. The mean numbers of monomers per oligomer are determined to be 17 $\pm$ 2 and 31 $\pm$ 6 for the 20% label density, 18 $\pm$ 1 and 36 $\pm$ 2 for the 15% label density, and 23 $\pm$ 3 and 44 $\pm$ 14 for the 10% label density.

number of monomers per oligomer was determined for both species (Fig. 4, *solid lines*). The experimental error is given by the uncertainty in the mean number of monomers per oligomer determined from the fitted binomial distributions and not by the width of the distribution, since aggregation is a stochastic process that always results in a distribution in the observed number of bleaching steps. The mean numbers of monomers per oligomer are determined to be 17 $\pm$ 2 and 31 $\pm$ 6 for the 20% label density, 18 $\pm$ 1 and 36 $\pm$ 2 for the 15% label density, and 23 $\pm$ 3 and 44 $\pm$ 14 for the 10% label density. The numbers of monomers that form an oligomer are, within the error bars, identical for the 20% and 15% label densities. To test whether the aggregation protocol reproducibly yields the same oligomers, we prepared a second batch of oligomers with a 15% label density. We found identical aggregation numbers (17 $\pm$ 2 and 35 $\pm$ 4) for this preparation (see Section S5 in the Supporting Material).

For the 10% label density, we observe deviations that can be explained by the low label density. For this label density, the mean number of bleaching steps for the smaller species of the dopamine-induced oligomers is <2. In this case, $>15\%$ of the oligomers do not contain a fluorescent label due to the stochastic nature of the aggregation process and are hence not included in the histogram of bleaching steps. This will result in the observed overestimation of the aggregation number. This severe overestimation of the aggregation number of the smaller species also results in an overestimation of the number of monomers in the larger species. The uncertainty in the number of monomers per oligomer for the 10% label density is also reflected by the correspondingly large experimental error compared to that found for the 15% label density.

For the 20% label density, we find a small deviation in the larger, second species compared to the 15% label density, which can be attributed to the large number of bleaching steps. The mean number of bleaching steps for the larger species of the dopamine-induced oligomers is >7, which results in ~10% of the oligomers containing >10 fluorescent labels. As we have shown previously, 10 bleaching steps is at the limit of what can still be accurately determined from a time trace (12). This results in the observed underestimation of the aggregation number for the larger species, which is also reflected by the larger experimental error compared to the error found for the 15% label density.

The presence of oligomers with no labels, and oligomers with too many labels, limits the range of label densities within which the technique of single-molecule photobleaching in combination with substoichiometric labeling can be used. The optimal label density depends on the aggregation number and the heterogeneity of the protein aggregates. As explained above, if the mean number of labels is <2, $>15\%$ of the oligomers do not contain a fluorescent label. Therefore, as an estimate, the lowest suitable label density follows from the rule that the mean number of bleaching steps, and hence the mean number of labels, needs to be at least 2. The mean number of bleaching steps is given by the product of the label density and the aggregation number. For the oligomers studied here, using the smallest aggregation number found for the 15% label density of 18 monomers/oligomer as a reference value, the lowest suitable label density is ~11%.

On the other hand, if the mean number of labels is about 8, $>15\%$ of the oligomers will contain too many labels and will not be analyzable. Therefore, the highest suitable label density can be estimated according to the rule that the mean number of bleaching steps should be ~8. For the oligomers studied here, taking the largest aggregation number found for the 15% label density of 36 monomers/oligomer, the highest suitable label density is ~22%.

We cannot, however, resolve a small heterogeneity of the number of monomers per oligomer within each species. Such a range of species would result in a broadening of the histogram of bleaching steps compared to the fit, which is very difficult to observe if a sum of binomials is fitted. Furthermore, adding more species to the fit did not improve the fit or yield distinctly different values, indicating that possible additional species must have aggregation numbers similar to the species already found. Therefore, the largest heterogeneity within each species is given by the uncertainty in the mean number of monomers per oligomer.

Our data clearly show that dopamine-induced oligomers formed under these conditions are present in two species. As a control, we also analyzed oligomers that are formed under identical aggregation conditions but in the absence of dopamine. We find that the oligomers formed in the absence of dopamine also display a bimodal distribution but with clearly different aggregation numbers (see Section S6 in the Supporting Material). Our single-molecule photobleaching experiments indicate that oligomer formation depends much on the experimental conditions. Our previous published work (12), where aS was aggregated at high concentrations and for long incubation times yielded a single species of aggregation number ~30. The protocol used here, using low aS concentrations and short aggregation times in the presence or absence of dopamine gave rise to distinctly different oligomers. Dopamine clearly has a specific effect on oligomer formation, leading to larger aggregation numbers for both detectable species. It has been reported that dopamine is incorporated into oligomers (20). The difference in oligomer aggregation number observed in the presence of dopamine likely results from the dopamine-mediated changes in interactions between the aS monomers. There is considerable discussion about whether dopamine forms covalent or noncovalent bonds with aS (16,18), although we are not in a position to distinguish between these possibilities with this technique. We note that the dopamine concentrations used are high compared to reported physiological concentrations (21), although it is reasonable to assume that the dopamine concentration is elevated in the substantia nigra.

The two species observed at shorter aggregation times, in both the presence and absence of dopamine, is a fundamentally different result than what we found for aS oligomers prepared using a different protocol based on a high concentration of aS and long aggregation times (12). For these oligomers, we found a single, well-defined species of oligomers. Section S7 in the Supporting Material shows the histogram of bleaching steps obtained for these oligomers, with a 15% label density fitted with both a single species and two species. Both fits give exactly the same aggregation number, with the two-species fit having a worse reduced χ-squared parameter. The finding from this work that dopamine-induced oligomers are present in two distinct species highlights that aS oligomers are indeed a heterogeneous family of aggregates in which the molecular details of the oligomers strongly depend on the conditions under which the oligomers form.

CONCLUSION

We have determined the aggregation number of dopamine-induced aS oligomers using the combination of single-molecule photobleaching and substoichiometric labeling. Using this combination of techniques, we are even able to distinguish multiple distinct species present in the same sample and determine their respective aggregation numbers from a single histogram of bleaching steps. We show that dopamine-induced aS oligomers are present in two clearly different species. We found a small species consisting of 15–19 monomers per oligomer and a larger species of 34–38 monomers per oligomer. The small spread in the number of monomers determined per species might reflect small variations in the number of monomers per oligomer. However, the current data do not allow us to resolve the details of the aggregation number within the individual species. Interestingly, the numbers found suggest that the larger species might be a dimer of the smaller species. We do not see any indications of the presence of even larger assemblies, such as tetramers, which should be detectable at the 10% label density. The relative fractions obtained from the fit indicate that both species are present in about the same fraction.

Our results show that aS forms oligomers of a defined number of monomers and that there is not a wide distribution in the number of monomers per oligomer. Depending on the conditions, oligomers of different aggregation number are formed. The technique of single-molecule photobleaching of substoichiometrically labeled aS oligomers allows for the sensitive detection of subtle changes in the molecular composition and aggregation number, and makes possible a systematic study of the influence of the aggregation conditions on the aggregation number of the oligomers formed.

Our current finding of species of distinct aggregation number implies that oligomers organize in a stable structure, but that the structure depends on the aggregation conditions. Linking the well-defined aggregation number and specific structure of the oligomers to their cytotoxicity may allow insights into the cause of Parkinson's disease and provide specific targets for pharmaceutical intervention.

SUPPORTING MATERIAL

Seven figures are available at http://www.biophysj.org/biophysj/supplemental/S0006-3495(13)05798-6.

We thank Anja Stefanović for assistance with the dopamine-induced oligomer preparation protocol.

This work was financially supported by the Nederlandse Organisatie voor Wetenschappelijk Onderzoek (NWO) through the NWO-CW TOP program number 700.58.302. We also acknowledge support from the Stichting Internationaal Parkinson Fonds.

REFERENCES

1. Clayton, D. F., and J. M. George. 1998. The synucleins: a family of proteins involved in synaptic function, plasticity, neurodegeneration and disease. *Trends Neurosci.* 21:249–254.

2. Pakkenberg, B., A. Møller, …, H. Pakkenberg. 1991. The absolute number of nerve cells in substantia nigra in normal subjects and in patients with Parkinson's disease estimated with an unbiased stereological method. *J. Neurol. Neurosurg. Psychiatry.* 54:30–33.

3. Spillantini, M. G., M. L. Schmidt, …, M. Goedert. 1997. α-Synuclein in Lewy bodies. *Nature.* 388:839–840.

4. Danzer, K. M., D. Haasen, …, M. Kostka. 2007. Different species of α-synuclein oligomers induce calcium influx and seeding. *J. Neurosci.* 27:9220–9232.

5. Fink, A. L. 2006. The aggregation and fibrillation of α-synuclein. *Acc. Chem. Res.* 39:628–634.

6. Outeiro, T. F., P. Putcha, …, P. J. McLean. 2008. Formation of toxic oligomeric α-synuclein species in living cells. *PLoS ONE.* 3:e1867.

7. Winner, B., R. Jappelli, …, R. Riek. 2011. In vivo demonstration that α-synuclein oligomers are toxic. *Proc. Natl. Acad. Sci. USA.* 108:4194–4199.

8. Cappai, R., S. L. Leck, …, A. F. Hill. 2005. Dopamine promotes α-synuclein aggregation into SDS-resistant soluble oligomers via a distinct folding pathway. *FASEB J.* 19:1377–1379.

9. De Franceschi, G., E. Frare, …, P. P. de Laureto. 2011. Structural and morphological characterization of aggregated species of α-synuclein induced by docosahexaenoic acid. *J. Biol. Chem.* 286:22262–22274.

10. Näsström, T., T. Fagerqvist, …, J. Bergström. 2011. The lipid peroxidation products 4-oxo-2-nonenal and 4-hydroxy-2-nonenal promote the formation of α-synuclein oligomers with distinct biochemical, morphological, and functional properties. *Free Radic. Biol. Med.* 50:428–437.

11. van Rooijen, B. D., M. M. A. E. Claessens, and V. Subramaniam. 2009. Lipid bilayer disruption by oligomeric α-synuclein depends on bilayer charge and accessibility of the hydrophobic core. *Biochim. Biophys. Acta.* 1788:1271–1278.

12. Zijlstra, N., C. Blum, …, V. Subramaniam. 2012. Molecular composition of sub-stoichiometrically labeled α-synuclein oligomers determined by single-molecule photobleaching. *Angew. Chem. Int. Ed. Engl.* 51:8821–8824.

13. Ding, H., P. T. Wong, …, D. G. Steel. 2009. Determination of the oligomer size of amyloidogenic protein β-amyloid(1–40) by single-molecule spectroscopy. *Biophys. J.* 97:912–921.

14. Dukes, K. D., C. F. Rodenberg, and R. K. Lammi. 2008. Monitoring the earliest amyloid-β oligomers via quantized photobleaching of dye-labeled peptides. *Anal. Biochem.* 382:29–34.

15. Eggeling, C., J. Widengren, …, C. A. M. Seidel. 1998. Photobleaching of fluorescent dyes under conditions used for single-molecule detection: evidence of two-step photolysis. *Anal. Chem.* 70:2651–2659.

16. Rekas, A., R. Cappai, …, C. Le Lan Pham. 2014. Dopamine-induced α-synuclein oligomers. *In* Bio-Nanoimaging. V. N. Uversky and Y. L. Lyubchenko, editors. Academic Press, Boston, pp. 291–300.

17. Conway, K. A., J. C. Rochet, …, P. T. Lansbury, Jr. 2001. Kinetic stabilization of the α-synuclein protofibril by a dopamine-α-synuclein adduct. *Science.* 294:1346–1349.

18. Leong, S. L., C. L. L. Pham, …, R. Cappai. 2009. Formation of dopamine-mediated α-synuclein-soluble oligomers requires methionine oxidation. *Free Radic. Biol. Med.* 46:1328–1337.

19. Herrera, F. E., A. Chesi, …, P. Carloni. 2008. Inhibition of α-synuclein fibrillization by dopamine is mediated by interactions with five C-terminal residues and with E83 in the NAC region. *PLoS ONE.* 3:e3394.

20. Rekas, A., R. B. Knott, …, C. L. Pham. 2010. The structure of dopamine induced α-synuclein oligomers. *Eur. Biophys. J.* 39:1407–1419.

21. Mosharov, E. V., K. E. Larsen, …, D. Sulzer. 2009. Interplay between cytosolic dopamine, calcium, and α-synuclein causes selective death of substantia nigra neurons. *Neuron.* 62:218–229.